Electromagnetic behavior of in-situ synthesized MXene-based Ti<sub>3</sub>C<sub>2</sub>/TiO<sub>2</sub> composites

Kh. Zamani, M. Tavoosi\*, A. Ghasemi

Department of Materials Engineering, Malek-Ashtar University of Technology (MUT), Iran

Email: ma.tavoosi@gmail.com

Tel./Fax: +983134429844

**Abstract** 

The present work, set out with the aim of studying the effect of in-situ precipitation of TiO<sub>2</sub>

form Ti<sub>3</sub>C<sub>2</sub>T<sub>x</sub> MXene phase on the electromagnetic (EM) behavior of Ti<sub>3</sub>C<sub>2</sub>/TiO<sub>2</sub> composites.

In this regard, Ti<sub>3</sub>C<sub>2</sub>T<sub>x</sub> MXene phase was synthesized using HF acidic etching of Ti<sub>3</sub>AlC<sub>2</sub>MAX

phase and the in-situ precipitation of TiO<sub>2</sub> phase within Ti<sub>3</sub>C<sub>2</sub> sheets was followed by

controlled annealing in temperature range of 500-800 °C for 2 h. The phase and structural

characteristics of prepared composites were investigated using X-ray diffraction (XRD),

scanning electron microscope (SEM) and differential thermal analysis. The electromagnetic

behavior of samples was also analyzed using vector network analyzer (VNA). The results

showed that by performing the controlled annealing process of Ti<sub>3</sub>C<sub>2</sub>T<sub>x</sub> MXene phase, it is

possible to in-situ formation of TiO<sub>2</sub> phase and form the Ti<sub>3</sub>C<sub>2</sub>/TiO<sub>2</sub> composites. The

electromagnetic behavior of Ti<sub>3</sub>C<sub>2</sub>/TiO<sub>2</sub> composites is in direct relation with the percentage of

TiO<sub>2</sub> phase deposited within Ti<sub>3</sub>C<sub>2</sub> sheets during annealing process. The reflection loss (RL)

changed from -7.98 to -21.28 dB (within frequency range of 1-18 GHz) with increasing in

annealing temperature from 500 to 800 °C as well as increasing the size and percentage of

formed TiO<sub>2</sub> particles.

Keywords: MAX; MXene; In-situ; composite; Electromagnetic.

1

### 1. Introduction

High temperature electromagnetic wave absorbing materials thanks to their wide applications-have attracted the attention of scientific research societies. These materials have secured their place in communication means/devices, aerospace industries and electronic equipment [1]. Besides exhibiting high performance in waves absorbing, they should have very slight thickness, light weight and a wide frequency range [2]. Traditional wave absorbing materials including ferrites, metallic magnetic powders, conducting polymers, etc. faced limitations and did not meet these requirements. Hence, the development of new materials with the unique properties such as MAX and MXenes was accelerated [3].

MXenes are known by the general formula of  $M_{n+1}AX_n$  (n=1,2 or 3) generated by selective etching of MAX phase ceramics. In this formula, M is an intermediate metal, A is an element from group A (often an element from groups 3, 4 or 5 of periodic table), X is nitrogen or carbon and  $T_x$  representing superficial functional groups like -F, -OH, and -O [4, 5]. This group of materials, owing to their layered structure and a large number of native defects and chemically active surfaces, are most apt candidates for EM interference shielding and absorption applications [6].

Based on literatures, the shielding performance of MXenes can be improved by adding magnetic and dielectric reinforcing phases. However, dielectric reinforcement materials are more desirable for high temperature applications, as the magnetic properties of the material are lost at high temperatures [7-9]. In this regard, a large number of research works have been devoted to the investigation of MXene based composites containing dielectric materials [10]. Among the dielectric absorbent materials, TiO<sub>2</sub> is a suitable candidate for high temperature EM applications due to its stable dielectric property and low density. Also TiO<sub>2</sub> brings about an increase in Ti<sub>3</sub>C<sub>2</sub>T<sub>x</sub> MXene dielectric layers optimizing the impedance matching [11].

Moreover, TiO<sub>2</sub> can be deposited in-situ inside the MXene layers during a controlled annealing [12-14].

In this regard, Fan et al. [15] reported that the precipitation of TiO<sub>2</sub> nanoparticles from Ti<sub>3</sub>C<sub>2</sub>T<sub>x</sub> during annealing process has significant effects on EM absorption behaviors of prepared composites. In this research, the *RL<sub>min</sub>* of prepared Ti<sub>3</sub>C<sub>2</sub>T<sub>x</sub>/TiO<sub>2</sub> composite was reached to about 40.7 in matching frequency of 19.2 *GHz* (thickness 1.5 *mm*). In other work, Sun et al. [16] successfully grew TiO<sub>2</sub> particulate inside Ti<sub>3</sub>C<sub>2</sub>T<sub>x</sub> MXene layers using hydrothermal method and achieved the reflection loss of about 58.30 *dB* (1.75 *mm* thickness) in optimized composite. Reports presented by Gao et al. [18] and Yan et al. [17] also show the positive effects of the presence of TiO<sub>2</sub> on EM behavior of MXene based composites within band X boundary.

Despite the numerous studies about the preparation and different characteristics of MXene based composites, no coherent report has yet been presented on the exact effect of TiO<sub>2</sub> on the EM behaviors of these composites. So, this research focused on the in-situ preparation of TiO<sub>2</sub> phase within Ti<sub>3</sub>C<sub>2</sub> sheets during controlled annealing process of Ti<sub>3</sub>C<sub>2</sub>T<sub>x</sub> MXene phase. The most important goal of this work was to investigate the electromagnetic wave absorption behavior in the frequency range of L (1 to 2 *GHz*), S (2 to 4 *GHz*), C (4 to 8 *GHz*), X (8 to 12 *GHz*) and Ku (12 to 18 *GHz*) bands in the formed composites.

# 2. Experimental procedure

In this research, Ti<sub>3</sub>AlC<sub>2</sub>MAX powder with a purity of above 99% and a mean particle size of less than 10  $\mu m$  (REDOX company) were used as raw materials for the formation of MXene phase. The Ti<sub>3</sub>C<sub>2</sub>T<sub>x</sub> MXene phase was prepared using selective etching of Al from the Ti<sub>3</sub>AlC<sub>2</sub> MAX powder in the Hydrofluoric acid (HF) ( $\geq$ 40 wt%, analysis) [11]. In a typical synthesis process, 2 g of the MAX powders were slowly added to 50 mL of HF solution. The etching

process was continued for 24 h [19], while stirring proceeded with the help of a magnetic bar. Afterwards, the mixture was washed several times with deionized water whereupon centrifugation performed at 3500 rpm for 5 min per cycle. After the last centrifuge, the pH of the supernatant was around 7.0. Subsequently, the product was washed with alcohol and dried in a vacuum oven at 60  $^{\circ}C$  for 24 h [19]. The Ti<sub>3</sub>C<sub>2</sub>/TiO<sub>2</sub> composites were prepared during controlled annealing process of prepared Ti<sub>3</sub>C<sub>2</sub>T<sub>x</sub> MXene phase at temperature range of 500-800  $^{\circ}C$  for 2 h (under argon protective atmosphere).

Phase examinations of the obtained samples were done via X-ray diffraction (XRD) analysis by utilizing XRD device (PW3710, Phillips Co.) under voltage 40 kV and current 0.05 Ampere. Morphological characteristics of the powder samples were inspected through scanning electron microscopy (SEM) (VEGA-TESCAN-XMU, Czech Republic). The differential scanning calorimetry (DSC) analysis of the samples was also conducted using STA 409 PC/PG device (NETZSCH Co.), under argon gas protection with the heating rate of 20 °C/min. A PNA-5222A vector network analyzer (VNA) system was utilized for analyzing the electromagnetic waves absorption of the studied samples.

### 3. Results and discussion

The X-ray diffraction patterns of Ti<sub>3</sub>AlC<sub>2</sub> MAX phase before and after etching process at HF solution for 24 *h* are shown in Fig. 1. A glance at the peaks formed in Fig. 1 (a) at angles of 34.1, 36.8, 38.9, 41.9, and 74.2° based on the reference code (JCPDS:52-0875) indicates the formation of a high-purity Ti<sub>3</sub>AlC<sub>2</sub> MAX phase and there is no evidence of impurities in this sample. Fig. 1 (b) shows the XRD pattern of Ti<sub>3</sub>AlC<sub>2</sub> MAX phase after selective etching of Al in HF solution for 24 *h*. As can be clearly seen, the diffraction peaks corresponding to the Ti<sub>3</sub>AlC<sub>2</sub> phase completely disappear and the XRD pattern is formed at angles of 18.5, 35.9, 41.7 and 60.7° corresponding to the characteristic peaks of the Ti<sub>3</sub>C<sub>2</sub>T<sub>x</sub> MXene phase [11, 20]. The latter result is confirmed by the SEM micrographs illustrated in Fig. 2, where the

accordion-like multi-layered nano-flake  $Ti_3C_2T_x$  MXene is clearly visible. The result obtained from SEM image is consistent with those presented by Tong et al. [21].

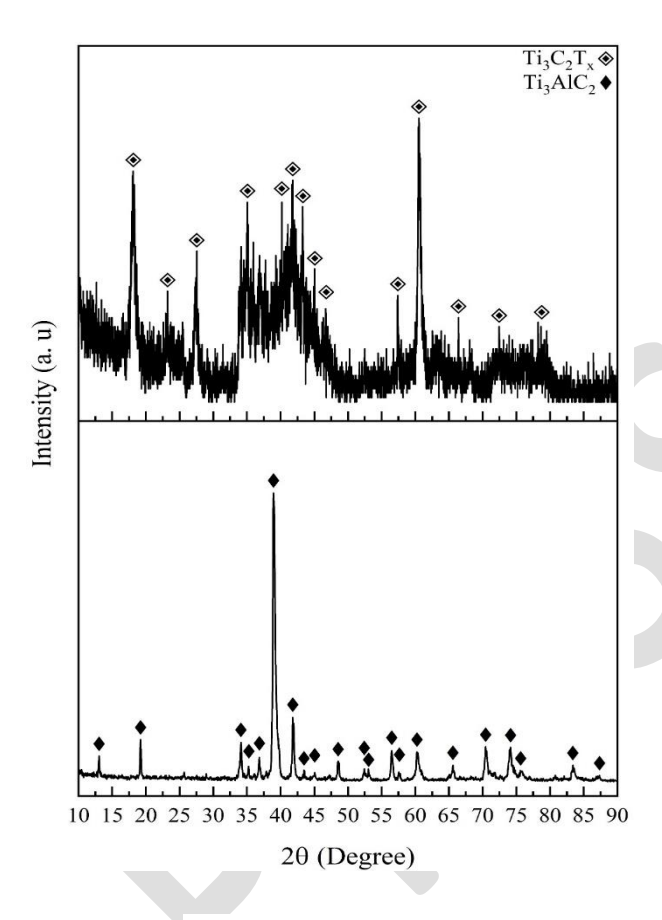


Fig.1. X-ray diffraction patterns of Ti<sub>3</sub>AlC<sub>2</sub> MAX phase a) before and b) after etching process in HF solution for 24 h.

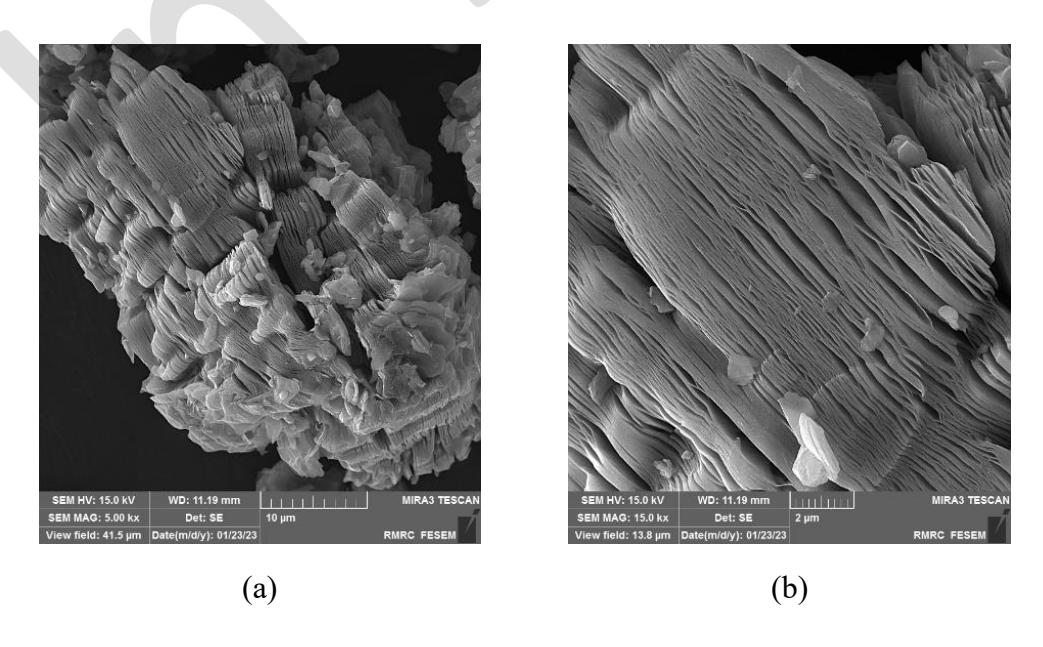


Fig.2. the SEM micrographs of Ti<sub>3</sub>AlC<sub>2</sub> MAX phase after etching process in HF solution for 24 *h* (at two different magnifications).

In order to study the thermal behavior of prepared Ti<sub>3</sub>C<sub>2</sub>T<sub>x</sub> MXene phase, the sample was examined using DSC technique under continuous heating. The DSC heating trace of this sample, in Fig. 3, reveals only one wide endothermic peak at temperature range of 500-800 °C. To analyze the phase transformation responsible for the endothermic peak, the Ti<sub>3</sub>C<sub>2</sub>T<sub>x</sub> MXene phase was annealed within 500, 600, 700 and 800 °C for 2 h and the samples were examined using XRD technique. The XRD patterns of annealed samples are presented in Fig. 4. As seen, during annealing process, the diffraction peaks intensity corresponding to MXene phase gradually decrease and several new peaks related to TiO<sub>2</sub> phase with anatase at 25.1, 37.5, 48.12, 54.7, and 69.56 ° angles (JCPDS:21-1272) and TiO<sub>2</sub> phase with rutile at 27.4, 36.06, 41.22, 54.32, and 56.7° angles (JCPDS:21-1276) structures appear in XRD patterns. This finding is in agreement with those reported by Lei et al. [22]. Therefore, the endothermic peak in Fig. 3 should be attributed to the precipitation of TiO<sub>2</sub> from the Ti<sub>3</sub>C<sub>2</sub>T<sub>x</sub> MXene phase. In fact, the presence of -OH and -O groups on the surface of Ti<sub>3</sub>C<sub>2</sub>T<sub>x</sub> causes thermodynamic instability of MXene and leads to the in-situ formation of TiO<sub>2</sub> deposits during annealing process [23, 24]. The following equations (1-5) can be proposed to explain the formation mechanism of Ti<sub>3</sub>C<sub>2</sub>/TiO<sub>2</sub> composite:

$$TiO_2(e^- + h^+) + Ti_3C_2 \to TiO_2(h^+) + Ti_3C_2(e^-)$$
 (1)

$$Ti_3C_2(h^+) + OH^- \to \bullet OH + TiO_2$$
(2)

$$Ti_3C_2(e^-) + O_2 \rightarrow \bullet O_2^- + TiO_2H_2O \bullet OH + Ti_3C_2$$
 (3)

$$TiO_2(h^+) + OH^- \to OH + TiO_2 \tag{4}$$

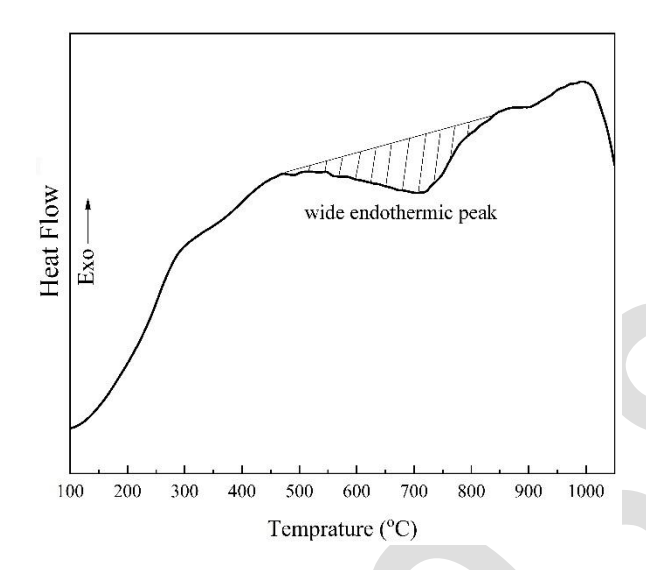


Fig.3. The DSC heating trace of Ti<sub>3</sub>C<sub>2</sub>T<sub>x</sub> MXene phase.

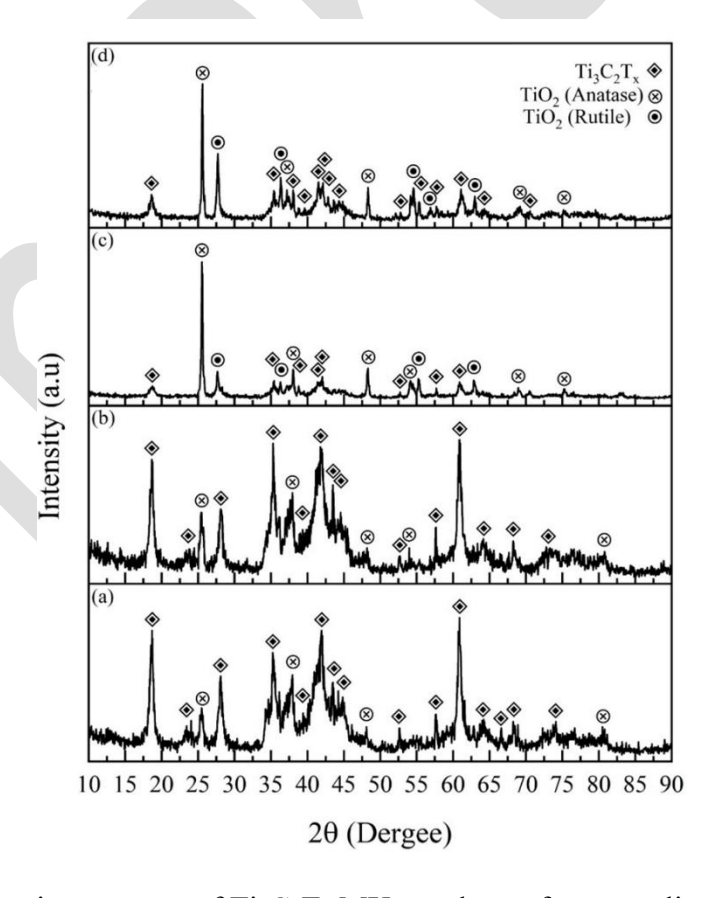
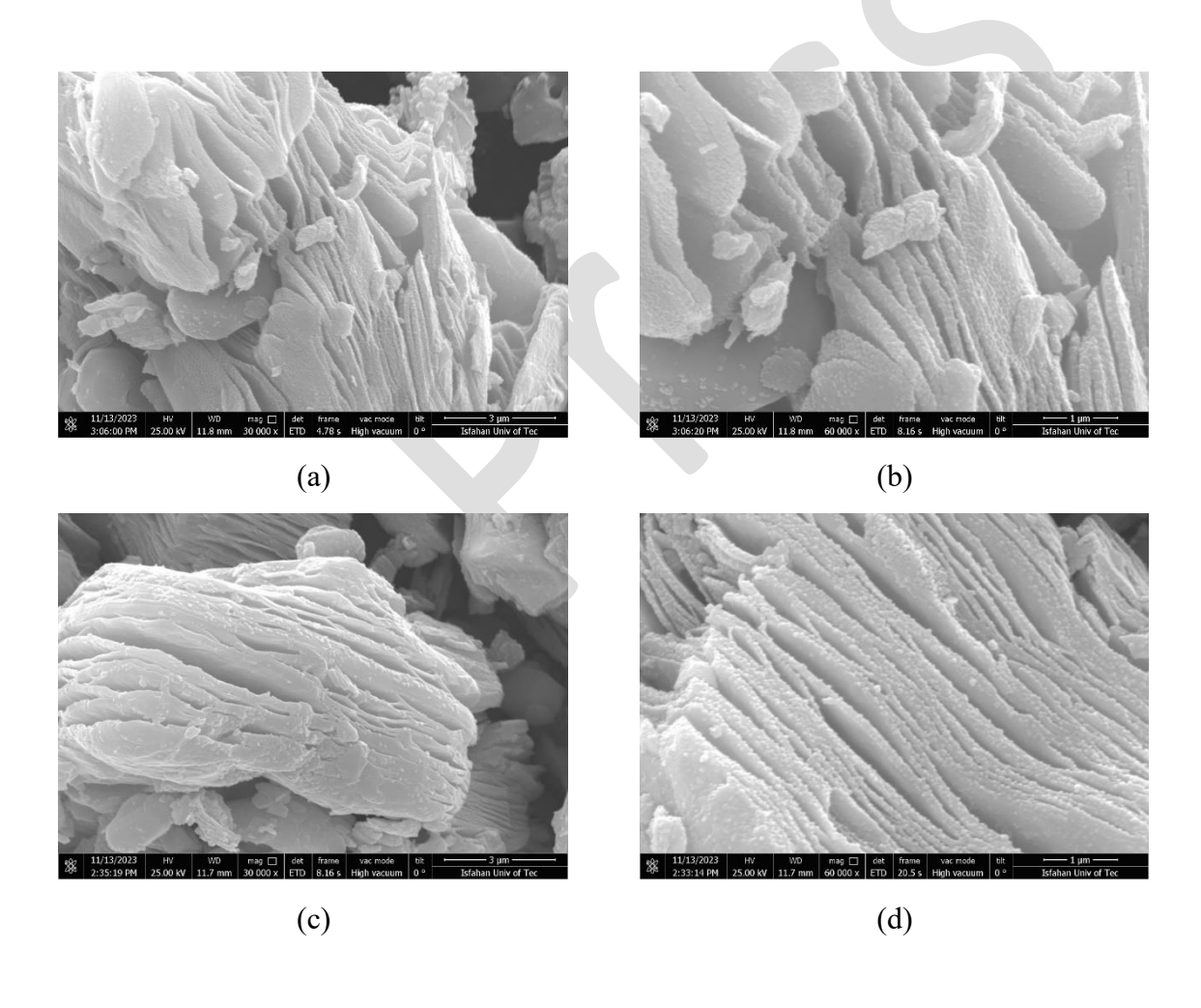


Fig. 4. X-ray diffraction patterns of  $Ti_3C_2T_x$  MXene phase after annealing process at, a) 500, b) 600, c)700 and d) 800  $^oC$  for 2 h.

As mentioned, the diffraction patterns presented in Fig. 4 well confirm the in-situ formation of Ti<sub>3</sub>C<sub>2</sub>/TiO<sub>2</sub> composites. This result is in agreement with the presented SEM micrographs of annealed samples at 500, 600, 700 and 800 °C in Fig. 5. Based on this figure, the nano-sized TiO<sub>2</sub> particles with unique distribution are formed on initial layers of MXene sheets. The morphology of formed TiO<sub>2</sub> nano-particles is closed to spherical and their size increases to about 180 *nm* with increasing annealing temperature.



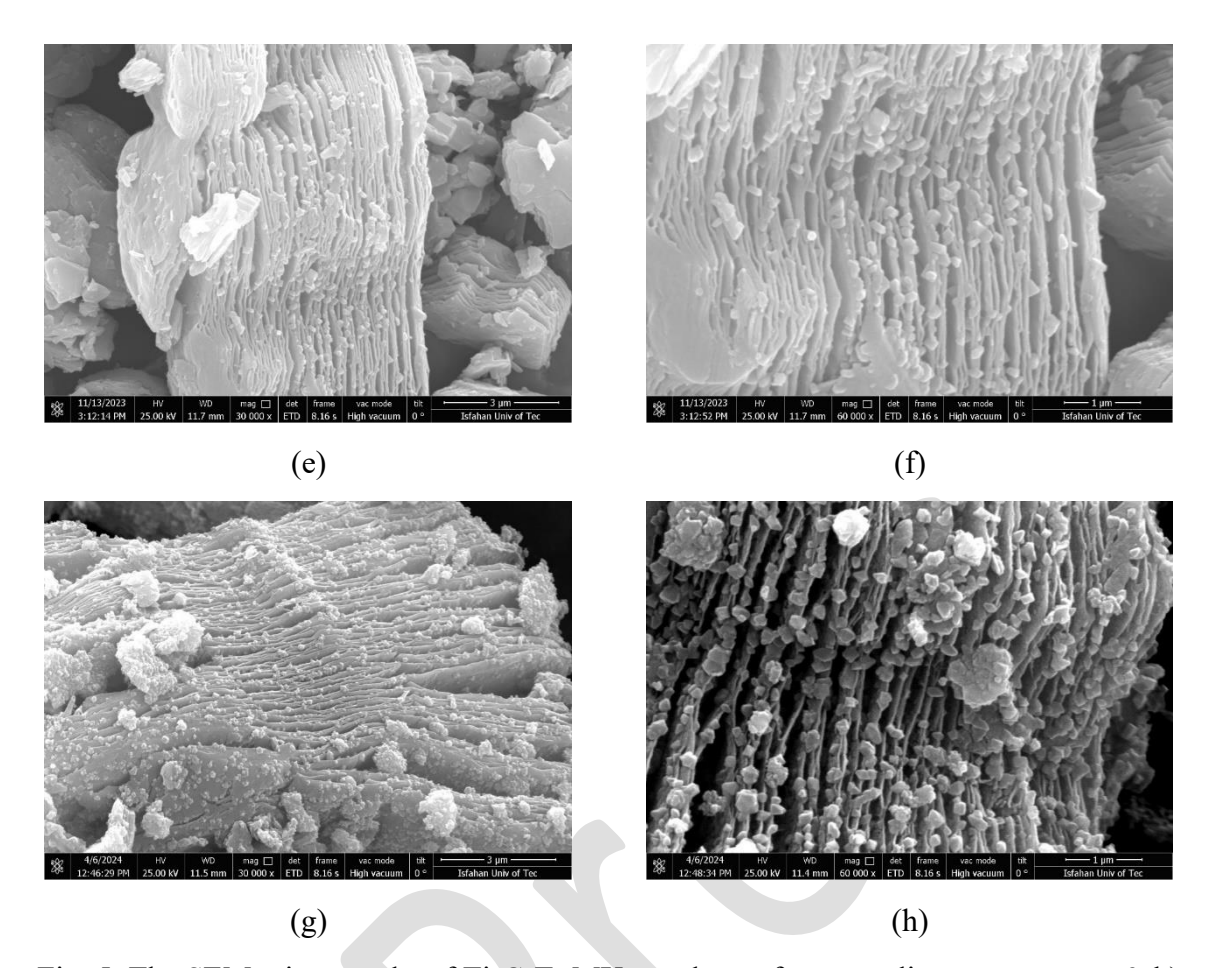


Fig. 5. The SEM micrographs of  $Ti_3C_2T_x$  MXene phase after annealing process at, a & b) 500, c & d) 600, e & f) 700 and g & h) 800  $^{o}C$  for 2 h.

Real parts of electrical permittivity ( $\varepsilon'$ ) and magnetic permeability ( $\mu'$ ) indicate electrical and magnetic energy storage potential. Whereas imaginary parts show rate of electrical and magnetic energy loss [25]. The real ( $\mu'$ ) and imaginary parts ( $\mu''$ ) of permittivity in prepared composites in this study are evaluated about 1 and 0, respectively as a result of the absence of magnetic components in composition. But, the changes in imaginary and real parts of electrical permittivity in relation to frequency (within 1-18 GHz) for prepared composites at different annealing temperatures are illustrated in Fig. 6. Based on this figure, several point can be concluded as:

- The pure  $Ti_3C_2$  MXene shows the highest values of real ( $\varepsilon'$ ) and imaginary part ( $\varepsilon''$ ) of electrical permittivity.

- By increasing the annealing temperature to 700 °C, the real and imaginary part of electrical permittivity decrease progressively. This point can be related to the change in MXene structure and precipitation of TiO<sub>2</sub> phase within the Ti<sub>3</sub>C<sub>2</sub> layers during annealing process.
- The changes in the imaginary and real parts of the electrical permittivity curves of the annealed samples at 700 and 800  $^{\circ}C$  are the same. This means that increasing the temperature further than 700  $^{\circ}C$  does not have a significant effect on the electrical permittivity of the resulting composites.
- The real and imaginary part of electrical permittivity of prepared composites follows a downward trend by increasing the frequency from 1 to 18 *GHz*. This is related to reductions in eddy currents losses [9].

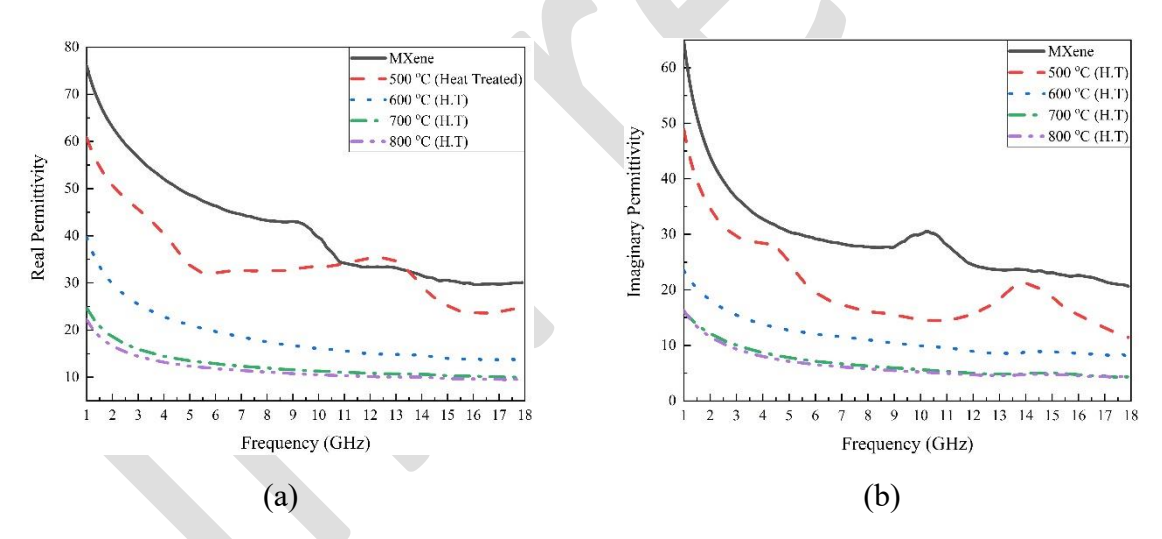


Fig. 6. The changes in a) imaginary and b) real parts of electrical permittivity in relation to frequency (within 1-18 *GHz*) for Ti<sub>3</sub>C<sub>2</sub>T<sub>x</sub> MXene phase before and after annealing process at different annealing temperatures.

The attenuation coefficient ( $\alpha$ ) and skin depth ( $\delta$ ) are important parameters for evaluating the dissipating capacity and the microwave absorption capability of an electromagnetic wave absorber, respectively. The higher the attenuation coefficient of an absorber, the more

electromagnetic wave energy can be converted into heat. The skin depth values also affect the ability to absorb EM waves. The thickness of the absorbing material must be greater than the skin depth in order to positively affect the absorption performance of EM waves. The changes in attenuation coefficient and skin depth versus the frequency for prepared composites are shown in Fig. 7. The presented results in Fig. 7 are calculated using the following equations [9, 17]:

$$\alpha = \frac{\sqrt{2\pi f}}{c} \times \sqrt{(\mu'' \varepsilon'' - \mu' \varepsilon') + \sqrt{(\mu'' \varepsilon'' - \mu' \varepsilon')^2 - (\mu' \varepsilon'' - \mu'' \varepsilon')^2}}$$
 (6)

$$\sigma = 2\pi f \,\varepsilon_0 \varepsilon'' \tag{7}$$

$$\delta = \sqrt{\frac{1}{\pi f \mu \sigma}} \tag{8}$$

Where, C is the speed of light in vacuum, f denotes the incident wave frequency,  $\sigma$  is conductivity,  $\varepsilon_0$  represents the electric permeability constant of the vacuum equal to  $854.8 \times 10^{-12}$  F/m.

Changes in damping constant relative to frequency for  $Ti_3C_2/TiO_2$  composites are displayed in Fig.7 (a). Based on equation (6), higher  $\varepsilon''$  result in a larger  $\alpha$  value. Therefore, the highest and lowest values of  $\alpha$  parameter correspond to pure  $Ti_3C_2T_x$  MXene and annealed samples at 800 °C, respectively. It should be noted that the value of parameter  $\alpha$  decreases with increasing frequency. In other words, composites prepared at high frequency have higher performance. According to the results presented in Fig. 7 (b), the values of  $\delta$  decrease abruptly in the range of 1–7 GHz, followed by an almost frequency-independent behavior. Based on this figure, it is quite evident that the maximum skin depth is related to  $Ti_3C_2/TiO_2$  composites annealed at 800 °C.

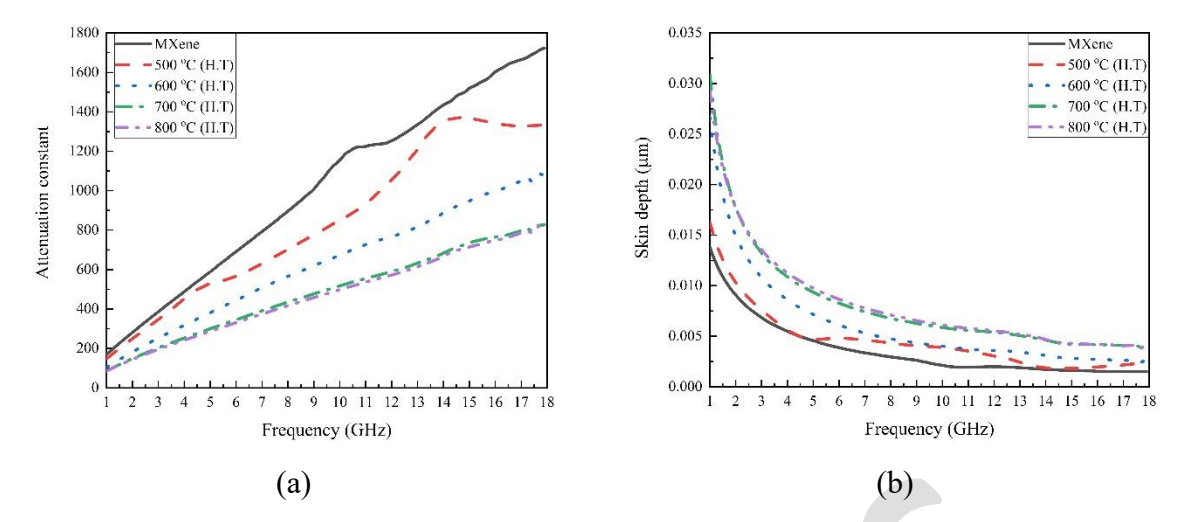


Fig. 7. The changes in a) attenuation constant and b) skin depth in relation to frequency (within 1-18 *GHz*) for Ti<sub>3</sub>C<sub>2</sub>T<sub>x</sub> MXene phase before and after annealing process at different annealing temperatures.

Reflection loss (RL) is a key parameter that characterizes the absorption characteristics of electromagnetic waves. When RL values are less than -10 dB, 90% of the EM wave energy is absorbed. EM wave absorption performance of prepared composites can be confirmed according to transmission line theory with RL value. It can be calculated by the correlation of complex permeability and complex permeability as follows [9]:

$$RL(dB) = 20 \log \left| \frac{Z_{in} - Z_0}{Z_{in} + Z_0} \right|$$
 (9)

$$Z_{in} = \sqrt{\frac{\mu_r}{\varepsilon_r}} \tanh\left[j\frac{2\pi ft}{c}\sqrt{\mu_r \varepsilon_r}\right]$$
 (10)

Where  $Z_{in}$  is the input characteristic impedance,  $Z_0$  denotes the impedance of free space, d stands for the thickness of the hybrid composite,  $\varepsilon_r$  shows the complex permittivity,  $\mu_r$  represents the complex permeability.

In this regard, the RL curves of prepared composites at different temperatures within frequency range 1-18 GHz (1-5 mm thicknesses) are illustrated in Fig. 8. As seen, best absorption behavior of EM waves belongs to the annealed sample at 800 °C with a thickness of 2 mm with the  $RL_{min}$  of about -22 dB at matching frequency of 12 GHz. Meanwhile, the weakest absorption behavior

of EM waves, with  $RL_{min}$  of about -5.51 dB at matching frequency of 8.95 GHz, is attributed to the pure Ti<sub>3</sub>C<sub>2</sub>T<sub>x</sub> MXene phase. Considering that the  $RL_{min}$  of composites prepared at temperatures below 500 °C (-7.98 dB at matching frequency of 7.88 GHz) is less than -10 dB, these materials are not suitable for EM absorption. In contrast, performing annealing process at higher temperatures has been able to increase the performance of the resulting structures in absorbing electromagnetic waves to an acceptable extent. As seen, the reflection loss (RL) changed from -7.98 to -21.28 dB (within frequency range of 1-18 GHz) with increasing in annealing temperature to about 800 °C. This result can be related to the increase in crystalline defects, reduction of interfaces and suitable percentage of TiO<sub>2</sub> within the Ti<sub>3</sub>C<sub>2</sub> sheets.

According to Fig. 8, matching frequencies of prepared composites shift to lower frequencies with increasing sample thickness. The reason is attributed to the spin matching at high frequencies. In fact, the studied samples in this work follow the law of quarter-wavelength weakening as follow [17]:

$$t_m = \frac{n\lambda_m}{4} = \frac{nc}{4f_m\sqrt{|\mu_r||\varepsilon_r|}} \tag{11}$$

In this equation,  $n = 1, 2, 3, f_m$  is the frequency corresponding to a particular RL peak, and  $\lambda_m$  denotes the wavelength at  $f_m$  [17]. Accordingly, the EM wave absorption function of the mentioned composites can be effectively adjusted by changing the thickness of the sample. The data present in Table 1 have been presented for comparing the synthesized samples and some advanced ceramics. Evidently, electromagnetic parameters are heavily affected by the chemical composition and microstructure. For example, the  $Ti_3C_2/TiO_2$  composites can be compared with  $Ti_3SiC_2/Al_2O_3$  and  $Ti_3C_2T_x/FC1$  [25, 26]. However,  $Ti_3C_2T_x/Fe_3O_4$  because of existence of magnetic losses ( $\mu'$ ,  $\mu''$ ) shows a better electromagnetic behavior [27].

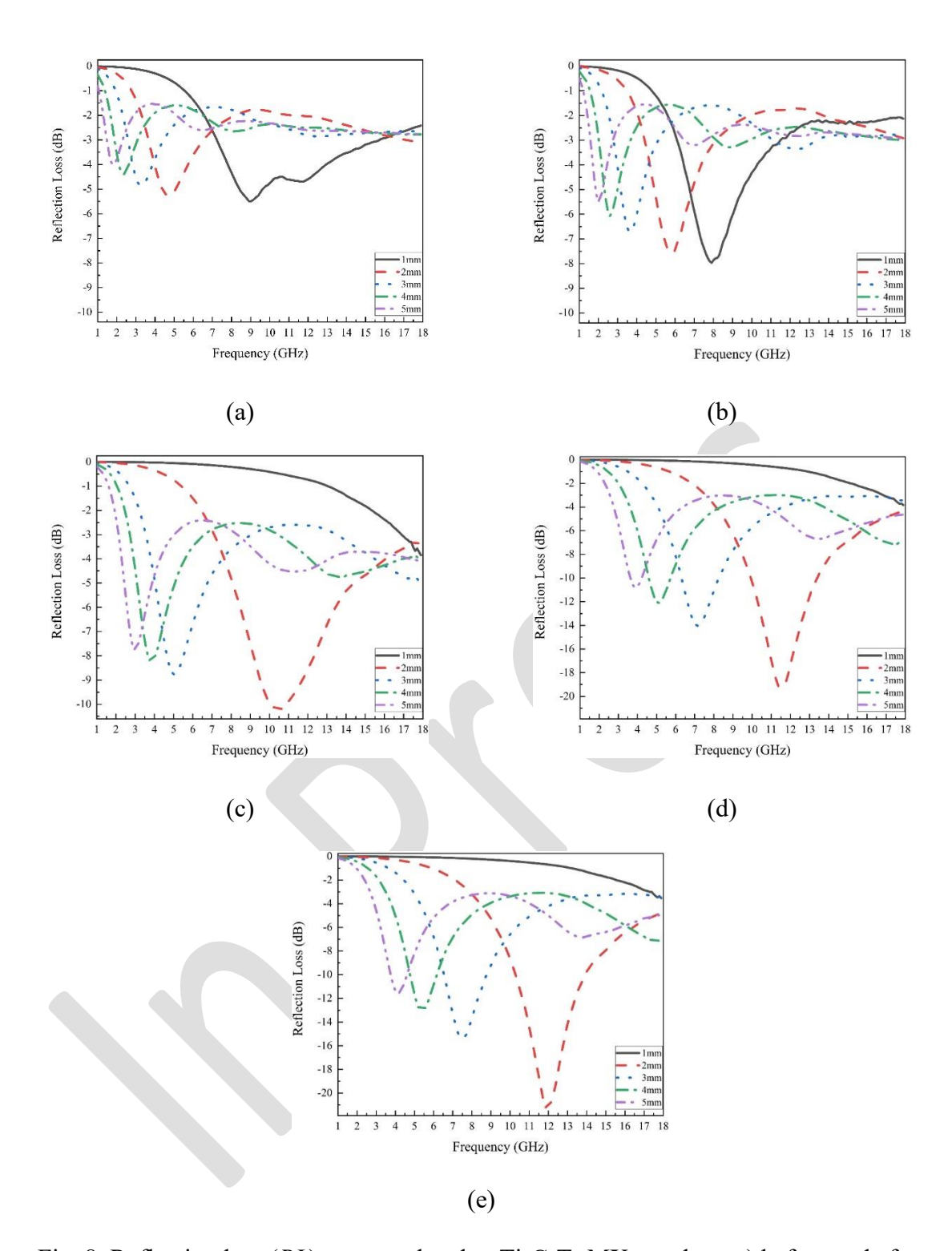


Fig. 8. Reflection loss (*RL*) curves related to Ti<sub>3</sub>C<sub>2</sub>T<sub>x</sub> MXene phase a) before and after annealing at b) 500, c) 600, d) 700 and e) 800 °C for 2 h.

Table 1. Comparison of EM wave absorbing properties of materials

Sample	RLmin (dB)	Layer thickness (mm)	Ref.
Ti <sub>3</sub> SiC <sub>2</sub> /Al <sub>2</sub> O <sub>3</sub>	-16.4	2	[25]
Ti <sub>3</sub> C <sub>2</sub> T <sub>x</sub> /FCl	-15.52	1	[26]
Ti <sub>3</sub> C <sub>2</sub> T <sub>x</sub> /Fe <sub>3</sub> O <sub>4</sub>	-57.2	3.6	[27]

### 4. Conclusion

The present work, set out with the aim of studying the effect of TiO<sub>2</sub> on the electromagnetic (EM) behavior of in-situ Ti<sub>3</sub>C<sub>2</sub>/TiO<sub>2</sub> composites. The results showed that by performing the controlled annealing process, it is possible to deposit the TiO<sub>2</sub> particles within the MXene phase and form the Ti<sub>3</sub>C<sub>2</sub>/TiO<sub>2</sub> composites in situ. The electromagnetic wave absorbing behaviors of Ti<sub>3</sub>C<sub>2</sub>/TiO<sub>2</sub> composites is in direct relation with the annealing temperature as a result of the insitu precipitation of TiO<sub>2</sub> within Ti<sub>3</sub>C<sub>2</sub> sheets. The reflection loss (RL) changed from -7.98 to -21.28 *dB* (within frequency range of 1-18 *GHz*) with increasing in annealing temperature as well as increasing the size and percentage of formed TiO<sub>2</sub> phase.

## Acknowledgments

I would like to thank Professor Ali Ghasemi for his invaluable feedback and reassurance, which influenced how I carried out my experiments, analyzed my results, and interpreted them.

### **Author contributions**

All authors have participated in (a) conception and design, or analysis and interpretation of the data; (b) drafting the article or revising it critically for important intellectual content; and (c) approval of the final version.

## **Conflicts of interest**

This manuscript has not been submitted to, nor is under review at, another journal or other publishing venue. The authors have no affiliation with any organization with a direct or indirect financial interest in the subject matter discussed in the manuscript. The authors have affiliations with organizations with direct or indirect financial interest in the subject matter discussed in the manuscript.

## Data and code availability

"Not Applicable"

## **Supplementary information**

"Not Applicable"

## Ethical approval

"Not Applicable"

# References

- [1] Wang, Z., Cheng, Z., Fang, C., Hou, X., Xie, L., "Recent advances in MXenes composites for electromagnetic interference shielding and microwave absorption". Composites Part A: Applied Science and Manufacturing, 2020, 136, 105956-105973.
- [2] Lim, K.R.G., Shekhirev, M., Wyatt, B.C., Anasori, B., Gogotsi, Y., She, Z.W., "Fundamentals of MXene synthesis". Nature Synthesis, 2022, 1(8), 601-614.
- [3] Heidarpour, A., Faraji, M., Haghighi, A., "Production and characterization of carbide-derived-nanocarbon structures obtained by HF electrochemical etching of Ti<sub>3</sub>AlC<sub>2</sub>". Ceramics International, 2022, 48 (8), 11466-11474.

- [4] Shahin, N., Kazemi, Sh., Heidarpour, A., "Mechanochemical synthesis mechanism of Ti<sub>3</sub>AlC<sub>2</sub> MAX phase from elemental powders of Ti, Al and C". Advanced Powder Technology, 2016, 27 (4), 1775-1780.
- [5] Aghamohammadi, H., Heidarpour, A., Jamshidi, R., Ghasemi, S., "Study on the chemical stability of the synthesized  $TiC_x$  in Ti-Al-C system after immersion in the  $HF+H_2O_2$  solution". Advanced Powder Technology, 2019, 30 (2), 393-398.
- [6] Pan, F., Yu, L., Xiang, Z., Liu, Z., Deng, B., Cui, E., Shi, Z., Li, X., Lu, W., "Improved synergistic effect for achieving ultrathin microwave absorber of 1D Co nanochains/2D carbide MXene nanocomposite". Carbon, 2021, 172, 506-515.
- [7] Wang, X., Zhao, C., Li, C., Liu, Y., Sun, S., Yu, Q., Yu, B., Cai, M., Zhou, F., "Progress in MXene-based materials for microwave absorption". Journal of Materials Science & Technology, 2024, 180, 207-225.
- [8] Guan, X., Yang, Z., Zhou, M., Yang, L., Peymanfar, R., Aslibeiki, B., Ji, G., "2D MXene nanomaterials: Synthesis, mechanism, and multifunctional applications in microwave absorption". Small Structures, 2022, 3(10), 2200102-2200125.
- [9] Ghasemi, A., Magnetic Ferrites and Related Nanocomposites, Elsevier, USA, 2022.
- [10] Chang, M., Li, Q., Jia, Z., Zhao, W., Wu, G., "Tuning microwave absorption properties of  $Ti_3C_2T_x$  MXene-based materials: Component optimization and structure modulation". Journal of Materials Science & Technology, 2023, 148, 150-170.
- [11] Kumar, A., Agarwala, V., Singh, D., "Microwave absorbing behavior of metal dispersed TiO<sub>2</sub> nanocomposites". Advanced Powder Technology, 2014, 25 (2), 483-489.
- [12] Liu, Z., Zhou, Y., Yang, L., Yang, R., "Green preparation of in-situ oxidized TiO<sub>2</sub>/Ti<sub>3</sub>C<sub>2</sub> heterostructure for photocatalytic hydrogen production". Advanced Powder Technology, 2021, 32 (12), 4857-4861.

- [13] F. Wang, C. Yang, M. Duan, Y. Tang, J. Zhu, TiO<sub>2</sub> nanoparticle modified organ like Ti<sub>3</sub>C<sub>2</sub> MXene nanocomposite encapsulating hemoglobin for a mediator-free biosensor with excellent performances, Biosensors and Bioelectronics 74 (2015) 1022-1028.
- [14] Tong, Y., He, M., Zhou, Y., Nie, S., Zhong, Q., Fan, L., Huang, T., Liao, Q., Wang, Y., "Three-dimensional hierarchical architecture of the TiO<sub>2</sub>/Ti<sub>3</sub>C<sub>2</sub>T<sub>x</sub>/RGO ternary composite aerogel for enhanced electromagnetic wave absorption". ACS sustainable chemistry & engineering, 2018, 6 (7), 8212-8222.
- [15] Fan, B., Shang, S., Dai, B., Zhao, B., Li, N., Li, M., Zhang, L., Zhang, R., Marken, F., "2D-layered Ti<sub>3</sub>C<sub>2</sub>/TiO<sub>2</sub> hybrids derived from Ti<sub>3</sub>C<sub>2</sub> MXenes for enhanced electromagnetic wave absorption". Ceramics International, 2020, 46 (10), 17085-17092.
- [16] Sun, X., Zhao, X., Zhang, X., Wu, G., Rong, X., Wang, X., "TiO<sub>2</sub> nanosheets/Ti<sub>3</sub>C<sub>2</sub>T<sub>x</sub> MXene 2D/2D composites for excellent microwave absorption", ACS Applied Nano Materials, 2023, 6 (15), 14421-14430.
- [17] Yan, H., Guo, Y., Bai, X., Qi, J., Lu, H., "Facile constructing  $Ti_3C_2T_x/TiO_2@C$  heterostructures for excellent microwave absorption properties". Journal of Colloid and Interface Science, 2024, 654, 1483-1491.
- [18] Gao, Y., Du, H., Li, R., Zhang, Q., Fan, B., Zhao, B., Li, N., Wang, X., Chen, Y., Zhang, R., "Multi-phase heterostructures of flower like Ni (NiO) decorated on two-dimensional Ti<sub>3</sub>C<sub>2</sub>T<sub>x</sub>/TiO<sub>2</sub> for high-performance microwave absorption properties". Ceramics International, 2021, 47 (8), 10764-10772.
- [19] Zamani, K., Tavoosi, M., Ghasemi, A., Gordani, G., "Electromagnetic characterization of MAX phase and MXene in Ti-Al-C ternary system", Materials Chemistry and Physics, 2024, 323, 129622-129632.

- [20] Tahir, M., "Nanoconfined Ti<sub>3</sub>C<sub>2</sub>@ in situ grown TiO<sub>2</sub> and ruthenium triphenylphosphine (Ru-II) coupled g-C<sub>3</sub>N<sub>4</sub> to construct RuP-Ti<sub>3</sub>C<sub>2</sub>@TiO<sub>2</sub>/EC<sub>3</sub>N<sub>4</sub> dual function nanocomposite for enhancing photocatalytic green hydrogen production". Chemical Engineering Journal, 2023, 476, 146680-146690.
- [21] Tong, Y., He, M., Zhou, Y., Zhong, X., Fan, L., Huang, T., Liao, Q., Wang, Y., "Electromagnetic wave absorption properties in the centimetre-band of Ti<sub>3</sub>C<sub>2</sub>T<sub>x</sub> MXenes with diverse etching time", Journal of Materials Science: Materials in Electronics, 2018, 29, 8078-8088.
- [22] Lei, B., Huang, X., Wu, P., Wang, L., Huang, J., Wang, Z., "Sandwich-like preparation of Ti<sub>3</sub>C<sub>2</sub>T<sub>x</sub>/CoFe/TiO<sub>2</sub> nanocomposites for high-performance electromagnetic wave absorption". Ceramics International, 2022, 48 (17), 25111-25119.
- [23] Yang, J.X., Yu, W.B., Li, C.F., Dong, W.D., Jiang, L.Q., Zhou, N., Zhuang, Z.P., Liu, J., Hu, J.Y., Zhao, H., "PtO nanodots promoting Ti<sub>3</sub>C<sub>2</sub> MXene in-situ converted Ti<sub>3</sub>C<sub>2</sub>/TiO<sub>2</sub> composites for photocatalytic hydrogen production". Chemical Engineering Journal, 2021, 420, 129695-129704.
- [24] Zhou, C., Wang, X., Luo, H., Deng, L., Wei, S., Zheng, Y., Jia, Q., Liu, J., "Rapid and direct growth of bipyramid TiO<sub>2</sub> from Ti<sub>3</sub>C<sub>2</sub>T<sub>x</sub> MXene to prepare Ni/TiO<sub>2</sub>/C heterogeneous composites for high-performance microwave absorption". Chemical Engineering Journal, 2020, 383, 123095-123104.
- [25] Dai, B., Zhao, B., Xie, X., Su, T., Fan, B., Zhang, R., Yang, R., "Novel two-dimensional Ti<sub>3</sub>C<sub>2</sub>T<sub>x</sub> MXenes/nano-carbon sphere hybrids for high-performance microwave absorption". Journal of Materials Chemistry C, 2018, 6, 5690-5697.
- [25] Zhang, X., Wang, H., Hu, R., Huang, C., Zhong, W., Pan, L., Feng, Y., Qiu, T., Zhang, C.J., Yang, J., "Novel solvothermal preparation and enhanced microwave absorption

properties of  $Ti_3C_2T_x$  MXene modified by in situ coated  $Fe_3O_4$  nanoparticles". Applied Surface Science, 2019, 484, 383-391.

[26] Yan, S., Cao, C., He, J., He, L., Qu, Z., "Investigation on the electromagnetic and broadband microwave absorption properties of Ti<sub>3</sub>C<sub>2</sub> Mxene/flaky carbonyl iron composites". Journal of Materials Science: Materials in Electronics, 2019, 30, 6537-6543.

[27] Zhao, D., Xia, S., Wang, Y., Wang, M., "High-performance microwave absorption properties of Ti<sub>3</sub>SiC<sub>2</sub>/Al<sub>2</sub>O<sub>3</sub> coatings prepared by plasma spraying". Applied Physics A, 2020, 126, 1-9.